IOP Publishing Journal of Physics B: Atomic, Molecular and Optical Physics

J. Phys. B: At. Mol. Opt. Phys. **40** (2007) 3467–3475 doi:10.1088/0953-4075/40/17/013

# Orientation and impact-parameter dependence of dissociative ionization of $H_2$ by slow ion impact

**F Afaneh[1], L Ph H Schmidt[2], M Schöffler[2], K E Stiebing[2], J Al-Jundi[1], H Schmidt-Böcking[2] and R Dörner[2]**

[1] Physics Department, The Hashemite University, PO Box 150459, Zarqa 13115, Jordan
[2] Institut für Kernphysik, Max-von-Laue-Str. 1, 60438 Frankfurt am Main, Germany

E-mail: afaneh@hu.edu.jo

Received 21 May 2007, in final form 28 June 2007
Published 28 August 2007
Online at stacks.iop.org/JPhysB/40/3467

**Abstract**

We have used the cold target recoil ion momentum spectroscopy imaging technique to investigate dissociative ionization of $H_2$ by 25 keV proton impact. A kinematically complete picture of the dissociative ionization dynamics for slow proton collision has been obtained. The results show a strong impact-parameter dependence of the fragmentation process of $H_2$. This clearly emerged in the energy distributions of the $H^+$ ions generated for different impact parameters. At large impact parameters the $H^+$ ions equally share the energy liberated in the collision whereas at small impact parameters, the energy sharing is quite asymmetric. We also observed a strong dependence of the electron emission on molecular alignment. The momentum distribution of the emitted electron generated for a fixed-in-space $H_2$ molecule displays that the electrons are more likely to be emitted perpendicular to the molecular axis.

## 1. Introduction

Dissociative ionization of small molecules by ion impact is of fundamental importance in many areas of science and technology, for example, in studies of astrophysical plasmas and upper planetary atmospheres or in studies of radiation damage of biological tissues [1–7]. Experimental studies of the ionization of small molecules by ion impact provide basic information for understanding of the fragmentation process by ion, electron or photon impact. In the case of electrons and photons the dissociation is mostly initiated by the creation of an inner-shell vacancy in the molecule [8–10]. For ion impact the fragmentation is mostly triggered by the removal of valence electrons from the molecule [11–15].

Depending on the collision velocity and on the charge state of the incident ion, dissociative ionization of molecules by ion impact results from electron capture as well as ionization processes. Except at very low collision energies, the collision time ($10^{-15}$–$10^{-17}$ s) is usually much shorter than the typical molecular dissociation, vibration and rotation time; therefore, the reaction can be separated into two steps: first, a transient molecular ion is produced during the collision event, the internal degrees of freedom of the molecule being frozen; second, if the excited molecular ion is unstable with respect to dissociation, fragmentation takes place. When dissociation occurs in a time short compared with the period of molecular rotation, the axial recoil approximation holds and the fragment ion trajectory reflects the orientation of the target molecule in space [16]. This can also be used to reconstruct the geometry of a more complex molecule by imaging the vector momenta of its fragments [17, 18].

Recent progress in the investigation of the dissociative ionization is due to the use of the coincidence multi-hit COLTRIMS (cold target recoil ion momentum spectroscopy) imaging technique [19–26] which has been mainly devoted to the momentum detection of the atomic fragments following molecular fragmentation. It was shown that coincident time-of-flight measurements with a position-sensitive multi-hit detector provide a complete three-dimensional image of the break-up process for each individual event. Thus the measured break-up pattern yields the complete information on the orientation of the molecular system with respect to the ion beam axis. A first quantitative measurement of vector correlation following ion-induced molecule fragmentation has been reported in pioneering experiments by Werner *et al* [27].

Measurements of fully differential cross sections for the dissociative ionization of the hydrogen molecule differential in the momentum of electrons, recoiling fragment ions and projectiles for slow incident protons at 25 keV are reported here. The measurements were carried out using the COLTRIMS imaging technique. The momentum vectors of both $H^+$ fragment ions and emitted electron have been measured in coincidence. In addition, the charge state of the outgoing projectile has been determined in coincidence too. Therefore, this study reports on a kinematically complete measurement of transfer ionization-induced dissociation of hydrogen molecules by proton impact at 25 keV.

## 2. Experimental setup

The experiment was performed at the electron cyclotron resonance (ECR) ion source of the Institut für Kernphysik of the Frankfurt University [28] using COLTRIMS [19, 20]. Briefly, the incoming 25 keV $H^+$ ion beam collimated to a small diameter of 1 mm intersects at right angles a supersonically cooled $H_2$ gas jet. After collision the charged projectiles are deflected electrostatically and the forward-scattered H neutrals are detected by a position-sensitive detector (PSD) consisting here of three channel plates and a delay line anode [21], located at 3.50 m from the target region. The fragment ions are extracted from the interaction region by means of a uniform dc electric field of 13 V $mm^{-1}$ perpendicular to the plane defined by the impacting ion and molecular beams. After the acceleration region, the fragments drift in a field-free region and reach a second PSD identical to the first one. On the opposite side the emitted electrons were accelerated for a distance of 15 mm, and then passed a drift tube of 40 mm length to be detected by a position-sensitive detector with an active diameter of 50 mm. This detector was shifted by 12 mm forward in the beam direction with respect to the reaction zone. The time-of-flights and positions of all collision products were simultaneously recorded with a 0.5 ns resolution 15-channel multi-hit time-to-digital converter (LeCroy TDC 3377). The TDC was operated in a common stop mode, i.e. where the signals were measured to a delayed common stop signal made by the coincidence between electron and recoil ion timing signals. Finally, the momentum vectors of both $H^+$ fragment ions and the emitted electron were calculated from the times-of-flight and the positions on the detectors. The projectile transverse momentum was determined from the impact position on the projectile detector [22, 23].

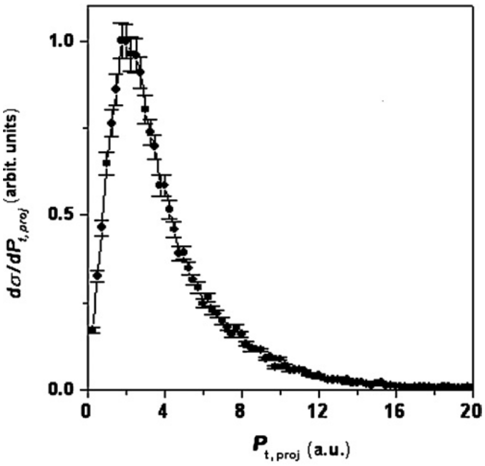

**Figure 1.** Transverse momentum of the scattered $H^0$ projectiles for dissociative transfer ionization of $H_2$ by 25 keV proton impact.

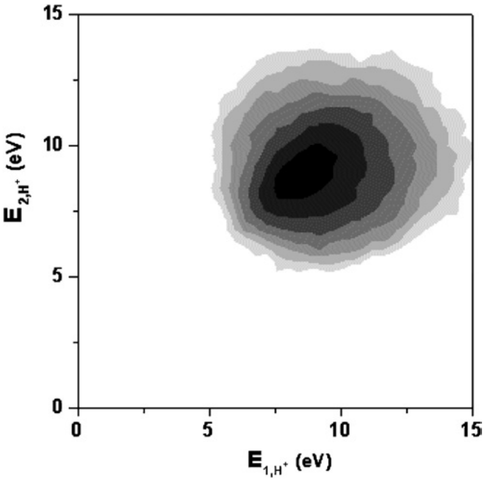

**Figure 2.** The energy of one $H^+$ plotted versus the energy of the other $H^+$.

## 3. Results and discussion

The removal of two electrons from $H_2$ automatically leads to the dissociation of the molecule,

$$H^+ + H_2 \rightarrow H^0 + H^+ + H^+ + e^-. \quad (1)$$

The $H^+$ ions as well as the emitted electron have been recorded in coincidence with the scattered projectile and their momentum vectors have been analysed. Figure 1 shows the transverse momentum of the scattered projectile. This transverse momentum can be related to an impact parameter. The distribution peaks at $P_\perp = 1.8$ au which, assuming an unscreened Coulomb potential, would correspond to an impact parameter of about 2.2 au ($P_\perp = 10$ and 20 au correspond to impact parameters in the range of 0.4 and 0.2 au, respectively).

Figure 2 shows the energy of one $H^+$ plotted versus the energy of the other $H^+$. The kinetic energy of the two ions in the final state is mainly provided by two sources, namely, the

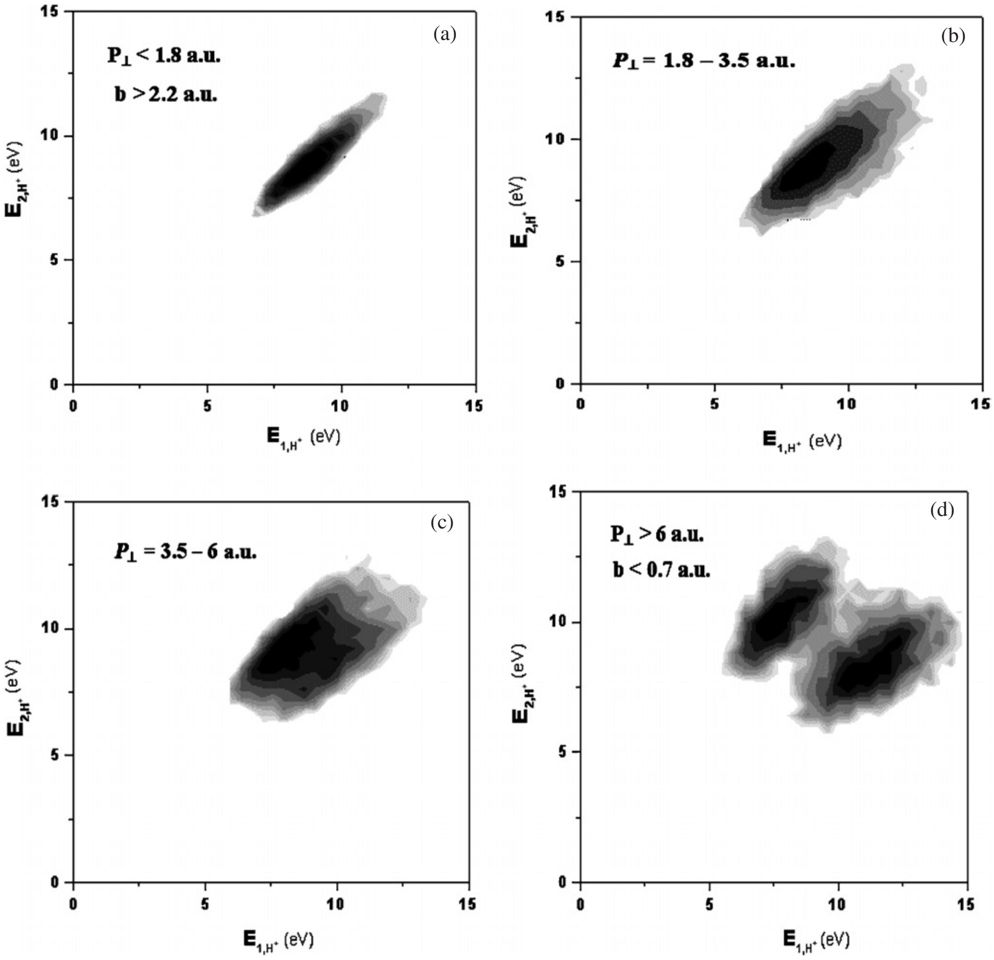

**Figure 3.** The energy of one $H^+$ fragment plotted versus the energy of the other $H^+$ for different ranges of projectile transverse momentum transfer, i.e. for different ranges of impact parameters. The transverse momentum transfer increases from (a) to (d); thus, the impact parameter decreases in the same direction.

collisional energy transferred from the projectile during the collision and the energy imparted to the fragment in the fragmentation process. To study the impact-parameter dependence of the fragmentation process, the energy of one $H^+$ is plotted versus the energy of the other $H^+$ in figure 3 for different ranges of projectile transverse momentum transfer. In these figures the transverse momentum transfer increases from (a) to (d) in figure 3; therefore, the impact parameter decreases in the same direction. These figures indicate a strong impact-parameter dependence of the fragmentation process. At large impact parameters ($P_\perp < 1.8$ au), the energy distribution of $H^+$ fragments is located close to the $E_{1,\mathrm{H}+} = E_{2,\mathrm{H}+}$ line as shown in figure 3(a). This indicates that the $H^+$ ions equally share the energy liberated in the explosion of the $H_2$ molecule and the energy transferred by the projectile to the ionic fragments is small. As the impact parameter decreases, the pattern becomes more and more different. The dominant feature in this case is that obviously the projectiles undergo a close collision with

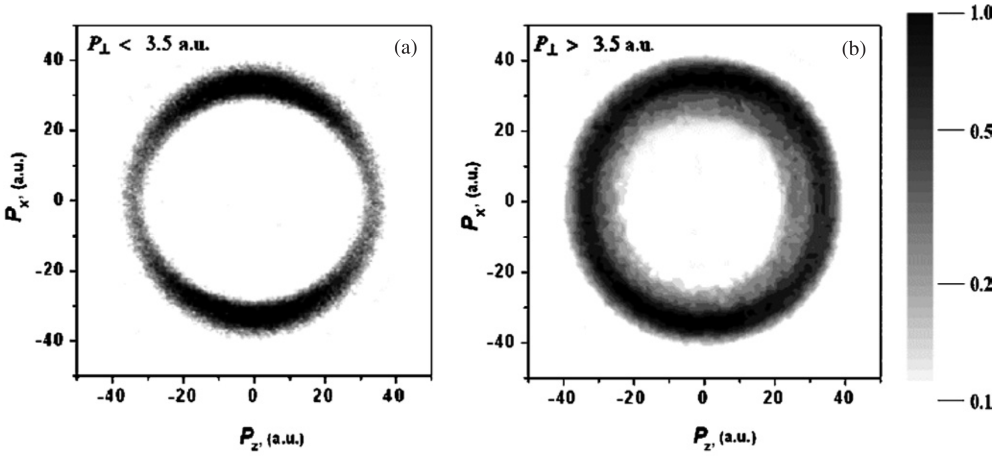

**Figure 4.** The $\boldsymbol{P}^{+}$ and $\boldsymbol{P}^{-}$ momentum distributions of $H^+$ fragments transformed into the scattering system where the $x'$ axis is defined by the transverse momentum transfer and the $z'$ axis coincides with the beam axis. The distributions are generated (a) for small transverse momentum transfer ($P_\perp < 3.5$ au) and (b) for large transverse momentum transfer ($P_\perp > 3.5$ au). The $\boldsymbol{P}^{+}$ momentum vector is fixed along the $x'$ axis.

one of the ionic fragments and transfer a non-negligible momentum, i.e. kinetic energy, to that fragment. At small impact parameters ($P_\perp > 6$ au) two different groups of $H^+$ fragments appear in the energy distribution presented in figure 3(d). The left group represents the $H^+$ fragments with lower kinetic energy than fragment 2. The right group is just the inverse case.

To understand the physics behind this effect the Jacobi coordinates have been used to present the momentum vectors for both fragments calculated in the laboratory frame. We define momenta $\boldsymbol{P}^{+} = 1/2(\boldsymbol{P}_1 + \boldsymbol{P}_2)$ and $\boldsymbol{P}^{-} = 1/2(\boldsymbol{P}_1 - \boldsymbol{P}_2)$, where $\boldsymbol{P}_1$ and $\boldsymbol{P}_2$ are the momenta of the fragment ions 1 and 2 in the laboratory system, respectively. Secondly, the $\boldsymbol{P}^{+}$ and $\boldsymbol{P}^{-}$ momenta are transformed to the scattering system $(x', z')$ where the $x'$ axis is defined by the momentum transfer of the projectile transverse to the beam axis and the $z'$ axis coincides with the beam axis. The $\boldsymbol{P}^{+}$ and $\boldsymbol{P}^{-}$ momenta are then generated for two different ranges of transverse momentum transfer. The resulted distributions are presented in figure 4. Both distributions show a ring which represents the Coulomb explosion process. It is interesting to note that the narrow Coulomb explosion ring appearing at the small momentum transfer becomes broader at large momentum transfer. This broadening ring results mainly from the vector addition of the momentum transferred to the centre-of-mass of the molecule. Such a result was also obtained by DuBois *et al* in their study of the impact velocity dependence of the fragmentation process of $D_2$ by slow highly charged xenon [29, 30].

The distribution of the total kinetic energy release (KER) of both $H^+$ fragments is shown in figure 5. The circles represent the energy release when the molecular axis is parallel to the beam direction; the squares show the same when the molecular axis points perpendicular to the beam direction. The results show that the total energy sum of both fragments at parallel orientation is larger than that at perpendicular orientation. To model these results, we use the reflection approximation [31], i.e. we calculate the KER by assuming Coulomb explosion from the $H_2$ ground state along the $H^+$–$H^+$ repulsive curve. Starting from a Gaussian distribution of internuclear distances (corresponding to a harmonic potential) yields the red curve in figure 5 while the more realistic Morse potential yields the blue curve. The removal

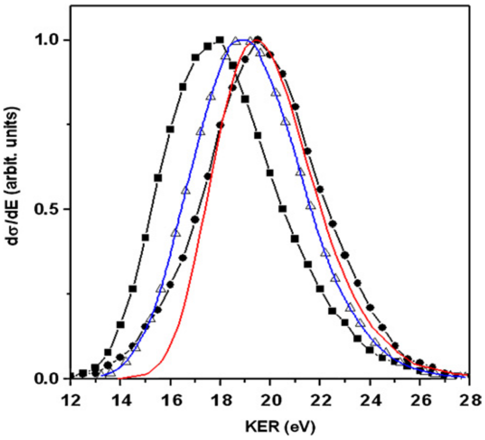

**Figure 5.** The total energy distribution of both $H^+$ fragments generated for parallel orientation (circles), i.e. parallel to the beam axis and perpendicular orientation (squares), i.e. perpendicular to it. The red curve shows the energy predicted starting from a distribution of internuclear distances of a harmonic oscillator potential. The blue curve shows the same from a Morse potential. The open triangles are the KER spectrum for the photo-fragmentation of a deuterium molecule measured by Weber *et al* [32].

(This figure is in colour only in the electronic version)

of both electrons by photodouble ionization was reported to yield perfect agreement with the blue curve [32]. Our ion impact results yield slightly higher or slightly lower KER depending on the molecular orientation. Slightly higher KER indicates an additional energy from the scattering of the projectile, as discussed above. Lower KER might indicate that the molecule somewhat dissociates ($\sim 10^{-15}$ s) before its Coulomb explosion ($\sim 10^{-14}$ s) [33]. Such effects are also seen for laser fragmentation of molecules [34–36].

In addition, the dependence on the molecular orientation of the emitted electron has been examined. The momentum distribution of the emitted electron is generated for a fixed-in-space $H_2$ molecule. The resulted distribution is presented in figure 6(a). In this figure the molecular axis is fixed as indicated and the momentum vector of the electron has been plotted. The distribution shows a pronounced angular distribution. The electrons are preferred to be emitted perpendicular to the molecular axis. This effect can be clearly seen by plotting the differential cross sections for the emitted electrons as a function of the polar electron emission angle relative to the molecular axis as shown in figure 6(b). The same result has been obtained in the momentum distribution of $H^+$ fragments generated for a fixed electron momentum vector as shown in figure 6(c). A similar behaviour has been observed by Dimopoulou *et al* in their studies of dissociative and non-dissociative single ionization of $H_2$ induced by 6 MeV proton impact [26]. Recently, the photon-induced molecule dissociation studies have shown similar orientation effects [32, 37, 38]. For instance, the angular distributions of the emitted electrons from the single-photon-induced fragmentation of the deuterium molecule measured by Weber *et al* [32] have revealed that the light field attempts to drive electrons towards a dipole pattern linked to its polarization axis, whereas the two-body Coulomb potential of the molecule tends to favour electrons escaping perpendicular to its axis. This result has received a strong support from the recent theoretical studies on the double photoionization of $H_2$ [39–41]. It has been suggested that the ground-state electron momentum distribution in the molecule is the possible reason for the preferred emission perpendicular to the molecular axis. Because the electronic

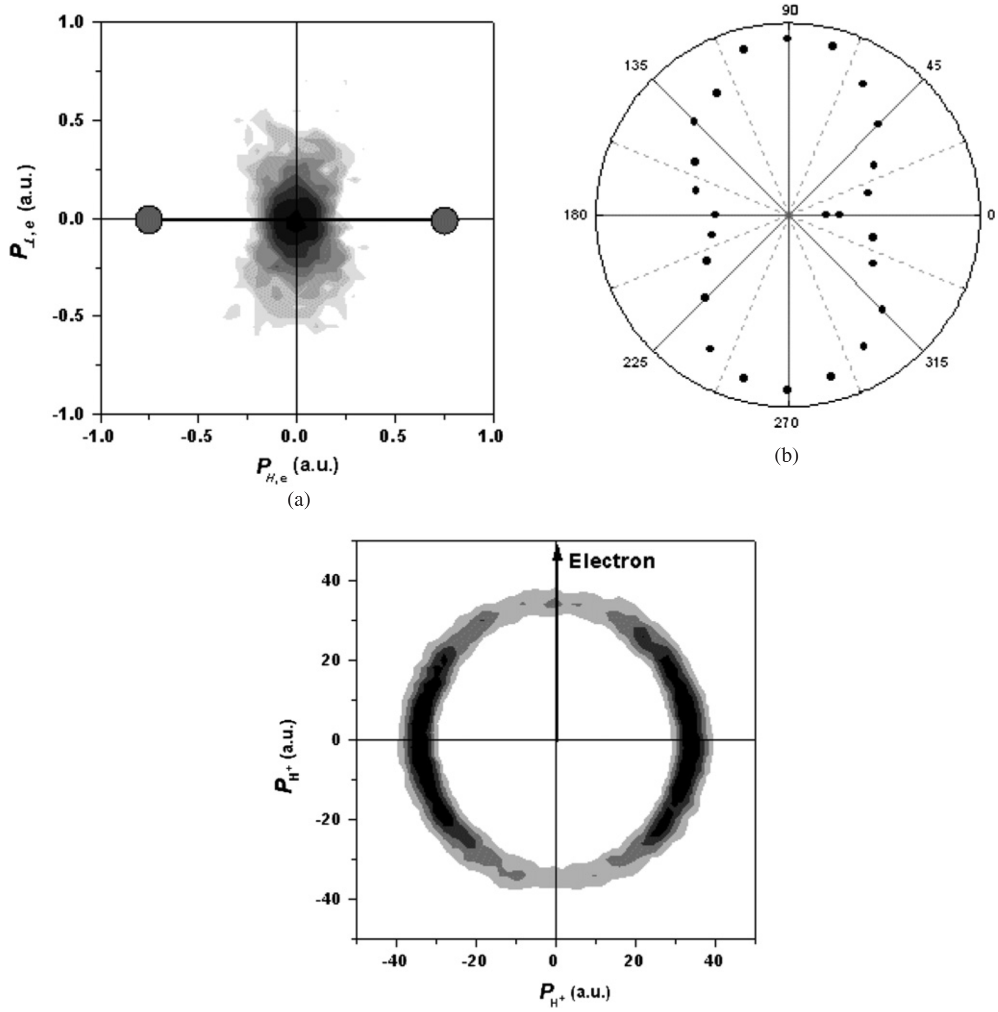

(a) (b) (c)

**Figure 6.** (a) The momentum distribution of the emitted electron generated for a fixed-in-space $H_2$ molecule. (b) The differential cross sections for the emitted electrons as a function of the polar electron emission angle relative to the molecular axis. (c) The momentum distribution of $H^+$ fragments generated for a fixed electron momentum vector.

wavefunction is elongated along the internuclear axis in configuration space, the momentum space wavefunction forms a peak perpendicular to the molecular axis [37]. Moreover, in their study of the internuclear distance dependence of this orientation effect, Horner *et al* [39] have found that this effect becomes more pronounced as the molecule is stretched.

## 4. Conclusions

The COLTRIMS imaging technique has been applied for the investigation of dissociative ionization of $H_2$ by proton impact. We obtained a kinematically complete picture of the ionization dynamics for slow proton impact, which is unprecedented in completeness and detail. The energy distributions of the $H^+$ ions generated for different ranges of impact parameters reveal a strong impact-parameter dependence of the fragmentation process of $H_2$. At large impact parameters the $H^+$ ions equally share the energy liberated in the collision. At small impact parameters, different features have been appeared which show an asymmetric energy sharing. A strong dependence of the dissociative ionization process on the molecular orientation has been observed. In addition, the momentum distribution of emitted electrons generated for a fixed-in-space $H_2$ molecule displays that the electrons are preferably emitted perpendicular to the molecular axis.

## Acknowledgments

FA gratefully acknowledges support from the Hashemite University, the DAAD, the DFG and the TWAS. The authors thank RoentDek GmbH for the preparation of the position sensitive detectors and other technical equipment. This work is supported by DFG, the Hashemite University, DAAD, RoentDek GmbH and TWAS.

## References

[1] Latimer C J 1993 *Adv. At. Mol. Opt. Phys.* **30** 105
[2] Kirby K P 1993 *The Physics of Electronic and Atomic Collisions (Proc. 18th ICPEAC)* ed T Andersen, B Fastrup, F Folkman and H Knudsen (New York: AIP) pp 48–58
[3] Rudd M E, Goffe T V, DuBois R D and Toburen L H 1985 *Phys. Rev.* A **31** 492
[4] Tawara H, Tonuma T, Shibata H, Kase M, Kambara T, Be S H, Kumagai H and Cono I 1986 *Phys. Rev.* A **33** 1385
[5] De Vries J *et al* 2003 *Phys. Rev. Lett.* **91** 053401
[6] Schlatholter T *et al* 2004 *Int. J. Mass Spectrom.* **233** 173
[7] Bodewits D *et al* 2005 *Nucl. Instrum. Methods* B **235** 358
[8] Märk T D 1985 *Electron Impact Ionization* ed T D Märk and G H Dunn (New York: Springer)
[9] Baltzer P *et al* 1994 *J. Phys. B: At. Mol. Opt. Phys.* **27** 4915
[10] Nenner I and Morin P 1995 *VUV and Soft X-Ray Photoionization Studies in Atom and Molecules* ed U Becker and D A Shirleydr (London: Plenum) chapter 9
[11] DuBois R D *et al* 2000 *Europhys. Lett.* **49** 41
[12] Frémont F *et al* 2000 *J. Phys. B: At. Mol. Opt. Phys.* **33** L249
[13] Tarisien M *et al* 2000 *J. Phys. B: At. Mol. Opt. Phys.* **33** L11
[14] Afaneh F *et al* 2002 *J. Phys. B: At. Mol. Opt. Phys.* **35** L229
[15] Siegmann B *et al* 2001 *Rev. Phys.* A **65** 010704
[16] Zare R N 1967 *J. Chem. Phys.* **47** 204
[17] DeFanis A *et al* 2004 *Phys. Rev.* A **69** 022506
[18] Muramatsu Y *et al* 2002 *Phys. Rev. Lett.* **88** 133002
[19] Dörner R, Mergel V, Jagutzki O, Spielberger L, Ullrich J, Moshammer R and Schmidt-Böcking H 2000 *Phys. Rep.* **330** 96
[20] Ullrich J, Moshammer R, Dorn A, Dörner R, Schmidt L Ph and Schmidt-Böcking H 2003 *Rep. Prog. Phys.* **66** 1463
[21] Jagutzki O *et al* 2002 *Nucl. Instrum. Methods* A **477** 244
[22] Afaneh F, Dörner R, Schmidt L Ph H and Schmidt-Böcking H 2005 *Nucl. Instrum. Methods* B **234** 431
[23] Afaneh F *et al* 2007 *J. Phys. B: At. Mol. Opt. Phys.* **40** 1745
[24] Schmidt L *et al* 2004 *Phys. Scr.* T **110** 379
[25] Laurent G *et al* 2006 *Phys. Rev. Lett.* **96** 173201
[26] Dimopoulou C *et al* 2004 *Phys. Rev. Lett.* **93** 123203
[27] Werner U *et al* 1997 *Phys. Rev. Lett.* **79** 1662
[28] Stiebing K *et al* 1996 *Nucl. Instrum. Methods* B **113** 34
[29] DuBois R D *et al* 2000 *Phys. Rev.* A **64** 022712
[30] Ali I *et al* 2000 *Phys. Rev.* A **62** 060701
[31] Le Rouzo H *et al* 1988 *Phys. Rev.* A **37** 1512
[32] Weber T *et al* 2004 *Nature* **431** 437

[33] Folkerts H O 1997 *PhD Thesis* University of Groningen
[34] Staudte A *et al* 2007 *Phys. Rev. Lett.* **98** 073003
[35] Alnaser A S *et al* 2004 *Phys. Rev. Lett.* **93** 183202
[36] Niikura H *et al* 2002 *Nature* **417** 917
[37] Weber Th *et al* 2004 *Phys. Rev. Lett.* **92** 163001
[38] Gisselbrecht *et al* 2006 *Phys. Rev. Lett.* **96** 153002
[39] Horner D A *et al* 2007 *Phys. Rev. Lett.* **98** 073001
[40] Foster M *et al* 2007 *Phys. Rev.* A **75** 062707
[41] Colgan J *et al* 2007 *Phys. Rev. Lett.* **98** 153001